

1 **Title:** Bio-optical signatures of *insitu* photosymbionts predict bleaching severity prior to thermal
2 stress in the Caribbean coral species *Acropora palmata*
3

4 **Running head:** AI-based, bio-optical bleaching prediction
5

6 **Authors:** Kenneth D. Hoadley (0000-0002-9287-181X)^{1,2}, Sean Lowry^{1,2}, Audrey McQuagge^{1,2},
7 Shannon Dalessandri^{1,2}, Grant Lockridge², Eleftherios Karabelas⁵, Courtney Klepac (0000-0002-
8 3935-8275)^{3,5}, Carly Kenkel (0000-0003-1126-4311)⁴, Erinn M. Muller (0000-0002-2695-
9 2064)^{3,5}

10

11 **Author affiliations:**

12 ¹University of Alabama, Tuscaloosa AL, USA

13 ²Dauphin Island Sea Lab, Dauphin Island AL, USA

14 ³Mote Marine Laboratory, Sarasota FL, USA

15 ⁴University of Southern California, Department of Biological Sciences, 3616 Trousdale Parkway,
16 Los Angeles, CA, 90089 USA

17 ⁵Mote Marine Laboratory, Summerland Key, FL, USA

18

19 **Corresponding Author:**

20 Kenneth D Hoadley, tel 251-861-2141 ext 7574, email: kdhoadley@ua.edu

21

22 **Abstract:** The identification of bleaching tolerant traits among individual corals is a major focus
23 for many restoration and conservation initiatives but often relies on large scale or high-
24 throughput experimental manipulations which may not be accessible to many front-line
25 restoration practitioners. Here we evaluate a machine learning technique to generate a predictive
26 model which estimates bleaching severity using non-destructive chlorophyll-a fluorescence
27 photophysiological metrics measured with a low-cost and open access bio-optical tool. First, a
28 four-week long thermal bleaching experiment was performed on 156 genotypes of *Acropora*
29 *palmata* at a land-based restoration facility. Resulting bleaching responses (percent change in
30 Fv/Fm or Absorbance) significantly differed across the four distinct phenotypes generated via a
31 photophysiology-based dendrogram, indicating strong concordance between fluorescence-based
32 photophysiological metrics and future bleaching severity. Next, these correlations were used to
33 train and then test a Random Forest algorithm-based model using a bootstrap resampling
34 technique. Correlation between predicted and actual bleaching responses in test corals was
35 significant ($p < 0.0001$) and increased with the number of corals used in model training (Peak
36 average R^2 values of 0.42 and 0.33 for Fv/Fm and absorbance, respectively). Strong concordance
37 between photophysiology-based phenotypes and future bleaching severity may provide a highly
38 scalable means for assessing reef corals.

39

40 **Keywords:** Coral bleaching, Coral photosymbiont phenotyping, Symbiodiniaceae photobiology,
41 Bio-optical bleaching prediction, High-throughput trait selection.

42 **Introduction:** Increasingly frequent coral bleaching events caused by ocean warming continue
43 to decimate reef systems across the globe (Hughes et al., 2017; Hughes et al., 2018). More than
44 ever before, coral reef conservation initiatives are focused on combating ecosystem loss through
45 the transplant of coral fragments onto impacted sites (Boström-Einarsson et al., 2020; Caruso et
46 al., 2021; Voolstra et al., 2021). Such efforts are meant to mitigate further ecosystem decline
47 while more permanent solutions to ocean warming can be found. The success of many coral
48 restoration initiatives, especially those on heavily impacted sites or areas expected to experience
49 severe environmental perturbations, is reliant on establishing colonies with more
50 environmentally resilient traits (Voolstra et al., 2020; Voolstra et al., 2021; Grummer et al., 2022;
51 Klepac et al., 2023). Indeed, high phenotypic variability in bleaching severity to thermal stress
52 exists within and across individual coral colonies (Parkinson et al., 2015; Kenkel & Matz, 2016),
53 and environments (Kenkel et al., 2013b; Palumbi et al., 2014; Barshis et al., 2018; Voolstra et al.,
54 2020) and likely reflects the outcome of various host and/or symbiont metabolic or cellular
55 pathways which together regulate the expulsion of symbiont cells (coral bleaching) from the host
56 tissue (Weis, 2008). However, initial identification of reef systems or individual coral colonies
57 with desirable traits such as thermal resilience is challenging (Parkinson et al., 2020), often
58 requiring expensive and time-consuming efforts not available to most front-line restoration
59 practitioners. New tools are needed that utilize our collective knowledge of coral physiology
60 and/or genetics to inform on key traits and facilitate colony selection for restoration activities.

61 The intracellular symbiotic algae (family: Symbiodiniaceae) are typified by high genetic
62 variability within and across individual species (LaJeunesse et al., 2018). In contrast, our
63 understanding of phenotypic variability across these algal species lags behind the genetics,
64 largely due to challenges in measuring cellular characteristics of algae living within the host

65 tissue. Nevertheless, coral thermal tolerance is often tied to specific symbiont species (Abrego et
66 al., 2008; Suggett et al., 2017; van Woesik et al., 2022) and further consideration is needed for
67 how functional traits link to underlying genetic variability across this algal lineage. Bio-optical
68 tools such as the Pulse Amplitude Modulated (PAM) fluorometer that measures algal-specific
69 traits such as variable chlorophyll *a* fluorescence have already provided critical insight into the
70 variability of thermal resilience across coral species, and individual colonies (Warner et al.,
71 1999; Voolstra et al., 2020; Cunning et al., 2021). However, more sophisticated fast repetition
72 rate fluorometers can offer greater insight into algal-centric thermal responses (Hoadley et al.,
73 2019; Hoadley et al., 2021) or functional trait variability (Suggett et al., 2015; Suggett et al.,
74 2022), leading the way towards further integration of these tools for coral research. Recently, we
75 developed a low-cost, multispectral, and fast repetition rate fluorometer capable of generating
76 over 1000 individual metrics within a short (11-minute) timespan and showcased its utility in
77 defining photosynthetic phenotypes across algal genera hosted by seven different coral species
78 under active restoration in the Florida Keys (Hoadley et al., 2023). Importantly, this work and
79 others suggest that algal-centric photo-physiological metrics are correlated with bleaching
80 severity and such information could provide a scalable means for identifying individual colonies,
81 coral species, or reef sites with high tolerance to thermal stress or other desirable traits. However,
82 further exploration is needed to understand if these highly dimensional and algal-centric
83 physiological metrics, along with machine-learning techniques can be effectively utilized to
84 develop predictive models for accurate trait-based selection of reef corals.

85 Here we evaluate the use of a machine learning technique to generate a predictive model
86 which estimates bleaching tolerance based solely on rapid and non-destructive chlorophyll-a
87 fluorescence, photo-physiological metrics measured with a low-cost and open access bio-optical

88 tool. First, a four-week long thermal bleaching experiment was performed on 156 genotypes
89 (genets) of *Acropora palmata* at a land-based restoration facility in the Florida Keys. Next,
90 correlations between algal photo-physiological metrics and bleaching response (percent change
91 in Fv/Fm or Absorbance at 675nm) were ranked and corals were randomly selected for use in
92 model training or testing. Evaluation was performed using a bootstrap technique to ensure robust
93 model performance across all coral genotypes. Prior studies that have used host genetic
94 information for predicting thermal tolerance found that accuracy improved dramatically when
95 environmental or information on the dominant symbiont type were also incorporated into their
96 model (Fuller et al., 2020). Our study extends this predictive concept by focusing on the
97 underlying phenotype of the symbiont as a tool for assessing coral tolerance. Artificial
98 intelligence-based techniques are increasingly applied within conservation and earth sciences
99 (Evans et al., 2012; Reichstein et al., 2019) and our study demonstrates its utility for trait-based
100 selection of reef corals using low-cost and rapid, bio-optical measurements of symbiont
101 physiology.

102 **Materials and Methods:**

103

104 **Coral selection and husbandry:** Mote's International Center for Coral Reef Research and
105 Restoration (MML-IC2R3) on Summerland Key, Florida contains approximately 60 land-based
106 raceways, supplied with filtered, UV sterilized, temperature-controlled, near-shore seawater and
107 maintained underneath 60% shade cloth canopies and corrugated clear-plastic rain-guards as
108 needed. Peak midday irradiance within these outdoor raceway aquaria was measured (Walz, 4pi
109 sensor) in 2021 (Hoadley et al., 2023) at $\sim 400 \mu\text{mol m}^{-2} \text{ sec}^{-1}$ under full sunlight, in the month of
110 May. Individual coral genotypes were pulled from Mote's restoration broodstock, with fragments
111 mounted to ceramic disks (Boston Aqua Farms, 3 cm diameter) using cyanoacrylate gel (Bulk
112 Reef Supply). Of the 156 *A. palmata* within the study, 30 were reared as sexual recruits from a
113 batch cross collected from the Upper Florida Keys in 2013 (29 genets) and 2015 (1 genet), 80
114 genets were the product of a batch cross sourced from Elbow/Biscayne in 2017, 42 genets were
115 the product of a batch cross sourced from the lower keys in 2020, and 4 were sourced as
116 collections directly from the reef Looe Key, Sand Key, WDR, Turtle reef) in 2018, 2021, 2021,
117 and 2014 respectively. Genotype identification was confirmed using single nucleotide
118 polymorphism loci (Kitchen et al., 2020). All coral fragments utilized in this study had been
119 propagated in Mote's *ex-situ* nursery and acclimated to the Climate and Acidification Ocean
120 Simulator (CAOS) system for 4 weeks prior to the start of experimental conditions.

121

122 **Phenotyping coral photosymbionts using chlorophyll *a* fluorescence:** Prior to experimental
123 bleaching, phenotypic measurements were derived (between March 31st – April 5th, 2022) from a
124 single coral fragment (ramet) per *A. palmata* genotype. Each fragment was dark acclimated for

125 20 minutes prior to fluorescence measurements. Importantly, the fragment used for capturing
126 phenotypic data is separate from the two fragments used to assess bleaching response metrics at
127 the end of the experiment. Within-genotype phenotypic variability is thus incorporated into our
128 overall design.

129 Fluorescence excitation in our phenotyping protocol was achieved using four excitation
130 wavelengths (415, 448, 470 and 505-nm) which preferentially target different photopigments
131 within the symbiotic algae. Fluorescence induction, which consists of the lowest initial
132 fluorescent measurement (F_o) to maximal fluorescence where the signal appears to plateau (F_m)
133 consisted of a series of brief excitation pulses, each 1.3- μ s long and followed by a 3.4- μ s dark
134 interval. For our samples, 32 flashlets was sufficient to reach a plateau in our induction curve
135 which was then used to calculate spectrally dependent F_o and F_m values, along with subsequent
136 metrics ((Φ_{PSII} , NPQ, and qP) as previously described in Hoadley et al., 2023. Additionally,
137 spectrally dependent excitation pressure over PSII (Q_m) was also calculated using the equation:

$$Q_m = 1 - \left(\frac{\text{quantum yield}}{\text{maximum quantum yield}} \right)$$

138 The excitation pressure over PSII equation is adapted from (Iglesias-Prieto et al., 2004) where
139 maximum quantum yield reflects the highest quantum yield value within the actinic light
140 protocol for a given sample and excitation wavelength. Power (irradiance in PAR) estimates
141 were used to determine the spectrally dependent functional absorption cross section of PSII
142 (σ_{PSII}) and antennae bed quenching (ABQ) according to previously published methods (Kolber et
143 al., 1998; Oxborough et al., 2012). A 300-millisecond fluorescent relaxation measurement
144 followed immediately after induction and utilized the same 1.3- μ s excitation flash but followed
145 by an exponentially increasing dark period (starting with 59- μ s). This induction and relaxation
146 process was run sequentially for each excitation color with a 200-millisecond delay in between

147 each run. Measured values reflect an average of 6 repeats per sampling time-point. Fluorescent
148 measurements were acquired during a 6-minute actinic light protocol which began with an initial
149 dark period, followed by three different light intensities ($200, 50, 400 \mu\text{mol m}^{-2} \text{ sec}^{-1}$) and a dark
150 recovery period (See PAR profile in Figure 1). A total of 28 evenly spaced sampling time points
151 were recorded during this actinic light protocol. Definitions and units for each of our 8 spectrally
152 dependent photo-physiological metrics calculated for each sampling time point in our
153 phenotyping protocol can be reviewed in Table 1.

154

155 **Thermal bleaching experiment:** Using the Climate and Acidification Ocean Simulator (CAOS)
156 system located at MML-IC2R3, a four-week long thermal bleaching experiment was performed
157 on the coral species, *Acropora palmata* (n=156 genotypes) from April 2-May 6 2022. All coral
158 fragments utilized in this study were acclimated for one month within the CAOS system prior to
159 the start of the experimental treatment. Control and heat treatments consisted of three shallow
160 raceways per treatment however, only a single fragment from one control and one high-
161 temperature raceway was utilized in the present study. Filtered seawater was continuously
162 supplied to each raceway (118 L hr^{-1}), with recirculating flow provided by a 5679 L hr^{-1} external
163 pump to supply the heat exchange system. Additional circulation was provided by four
164 submersible pumps (454 L hr^{-1} , Dwyer). All experimental systems were maintained underneath
165 60% shade cloth canopies and clear plastic rain guards with additional 60% shade cloth covers
166 added between 12:00 and 14:00 daily and experienced similar light levels as described above. At
167 the start of the experiment (April 2, 2022), the high-temperature raceway increased from 27.5°C
168 to 31.5°C by 0.5°C each day (8 days total). Control raceways remained at 27.5°C for the

169 duration of the 1-month experiment and high-temperature raceways remained at 31.5°C for 3
170 weeks and 32.0°C for the remainder of the 1-month experiment.

171

172 **Bleaching response metrics:** Measurements of the maximum quantum yield (Fv/Fm) using 448-
173 nm excitation and absorbance spectra were measured from all experimental fragments on
174 experimental days 39-42 (May 7-8th and 9-10th of 2022 for high temperature and control
175 treatment groups, respectively). Maximum quantum yield measurements were derived from
176 control and high temperature fragments after a 20-minute dark acclimation period and using the
177 same induction and relaxation protocol described above. Absorption-based measurements were
178 calculated on all coral fragments and achieved by measuring the reflectance spectra according to
179 previously established methods (Rodríguez-Román et al., 2006). A custom fiber optic cable
180 (Berkshire Photonics) coupled a white LED (Luxeon) to a USB2000 spectrophotometer (Ocean
181 Optics) for assessing spectral reflectance from all coral fragments in control and treatment
182 conditions. Reflectance measurements were normalized to a bleached *A. palmata* skeleton and
183 then converted into absorbance measurements which can serve as a non-invasive proxy for
184 changes in cell density/chlorophyll *a* content associated with coral bleaching (Rodríguez-Román
185 et al., 2006; Hoadley et al., 2016). Here, absorbance readings were measured at 675nm which
186 reflects the maximum chlorophyll-*a* absorbance band.

187

188 **Statistical analysis and bleaching response model generation:** All analyses were conducted in
189 R (v.3.5.1) (Team, 2017). For each coral genotype, bleaching response metrics (Fv/Fm and
190 absorbance at 675nm) were calculated as the percent change between control and high
191 temperature fragments (Figure 2). To minimize bias associated with high correlation between

192 certain photophysiological traits, a correlation matrix was first used to identify and then remove
193 individual metrics with high correlation ($\text{Rho} > 0.99$) to one another. All remaining
194 photophysiological metrics were then used to build a phenotypic dendrogram using the R
195 packages *pvclust* (Suzuki & Shimodaira, 2013) and *dendextend* (Galili, 2015). Resulting
196 dendrogram with 10,000 bootstrap iterations was then used to cluster individual genotypes into
197 four distinct clusters/phenotypes. Next, significant differences across our cluster-based
198 phenotypes for thermally-induced changes in absorbance and Fv/Fm were measured using a one-
199 way ANOVA with a Tukey-posthoc (all data fit assumptions of normality).

200 For assessing individual photophysiological metrics and their correlation to bleaching
201 response, all photo-physiological parameters were first screened for correlation with one another
202 (autocorrelation scores < 0.85 Rho) and then individually tested for correlation (spearman) with
203 bleaching response metrics (% change in absorbance and Fv/Fm). Only photo-physiological
204 metrics with significant ($p < 0.05$) correlation were included in Figure 4 (and Supplementary
205 tables S1 and S2).

206 Selecting which photo-physiological metrics to use to optimize a predictive bleaching
207 model is a critical step in our analytical pipeline. First, we screened for autocorrelation between
208 photophysiological metrics. Different correlation cutoff values were used when selecting metrics
209 for the assessment of % change in absorbance ($\text{Rho} > 0.85$) and Fv/Fm ($\text{Rho} > 0.75$) and are
210 based on resulting predictive performance. Next the *Boruta* R package (Kursa & Rudnicki, 2010)
211 was used to carryout feature selection on the remaining photophysiological metrics using a random
212 forest based assessment and prioritization. Resulting prioritized photophysiological metrics were
213 then used to develop separate models for predicting percent change in Fv/Fm and absorbance (at
214 675-nm) between control and treatment fragments. Randomly selected coral genotypes were

215 used in model training which consisted of using the Random Forest (RF) regression algorithm to
216 generate each model iteration. The strength of each individual RF model was then tested by
217 predicting bleaching response on 40 randomly selected colonies which were not used to generate
218 the model. Accuracy of each model was then measured using goodness of fit (R^2) and the root
219 mean square error (RMSE – describes the model error) between predicted and observed
220 bleaching responses (% change in Fv/Fm or absorbance). In addition to goodness of fit, the 40
221 ‘test’ corals were also ranked based on model predictions, and then the significance of actual
222 bleaching responses between the top and bottom 10 corals was statistically compared using a t-
223 test (Figure 4c,f). Accuracy of our RF models was evaluated as a function of the number of
224 corals (between 20 and 80) used for training, with each model repeated 100 times with randomly
225 selected corals (Bootstrap resampling technique). Importantly, outcomes were always tested
226 using 40 different corals (also randomly selected and separate from those used in training).
227 Bootstrap model scores enable us to evaluate stability and ensure performance was not biased
228 through inclusion/exclusion of a given coral genotype. Raw data along with analytical scripts for
229 generating Figures 2-5 are available via github ([khoadley/bleaching-prediction-2023](https://github.com/khoadley/bleaching-prediction-2023)).
230

231 **Results:**

232

233 **Bleaching Response:** Of the 156 *A. palmata* colonies that were evaluated for thermal stress
234 resilience, 32 were removed prior to the end of the two-month experiment due to extreme
235 bleaching (> 75%), while another 4 were not properly measured for photophysiology at the onset
236 of the experiment. Because these corals were either pulled from the experiment early, or were
237 missing critical data, they are not included in any downstream analyses or predictive bleaching
238 model testing shown here. For the remaining corals (n=120), the average percent change in
239 bleaching response metrics for Fv/Fm and absorbance was -14.58% ($\pm 45\%$ SD) and -23.36% (\pm
240 24% SD) respectively (Figure 2a,b). Correlation between the two bleaching response metrics was
241 evaluated using correlation ($R^2 = 0.016$, p value = 0.639) and reflects no significant linear
242 relationship (Figure 2c).

243

244 **Linking photo-physiological phenotypes with bleaching response:** Our photophysiology-
245 based dendrogram separated our 120 coral colonies into four distinct clusters with high bootstrap
246 support (Figure 3a). We next wanted to see if significant differences in bleaching sensitivity
247 existed between our four identified clusters/phenotypes. A one-way ANOVA with a Tukey-
248 posthoc found differences in the observed % change in absorbance and Fv/Fm across clusters (p
249 < 0.0001). For Absorbance, phenotype 1 displayed a significantly ($p < 0.044$) larger response to
250 thermal stress as compared to phenotypes 2 and 3 (Figure 3b). Phenotypes 2 ($p=0.01$) and 4
251 ($p=0.004$) also had a significantly larger response to thermal stress as compared to the most
252 resistant phenotype (phenotype3). For high-temperature induced changes in Fv/Fm, phenotype 1
253 had a significantly ($p < 0.002$) larger reduction as compared to phenotypes 2 and 4 (Figure 3c).

254

255 **Correlations between algal phenomics and bleaching response metrics:** A total of 896 photo-
256 physiological responses (8 photo-physiological responses * 4 excitation wavelengths * 28
257 sampling time points) were measured as part of our photo-physiologically based phenometric
258 assay. Using data from all 120 colonies, these photo-physiological metrics were first screened for
259 high-correlation ($\text{Rho} > 0.85$) with one another and then those remaining (311
260 photophysiological metrics) were directly tested for significant correlation ($p < 0.05$) with the
261 two individual bleaching metrics. Only 66 and 170 photo-physiological metrics were deemed to
262 have significant correlation with % change in Absorbance and Fv/Fm respectively. The absolute
263 range in Rho for significant metrics was between 0.179 - 0.448 for Absorbance and 0.184 - 0.455
264 for Fv/Fm (See Supplemental tables S1 and S2). Correlations were then plotted as a function of
265 which step in the actinic light protocol the phenometric values were derived (Figure 4a,c). For
266 both bleaching response metrics, significant correlations are predominantly made with
267 phenometrics derived immediately (within 10 seconds) after an increase in light intensity
268 (sampling time points 3-5 and 17-19), and strongly suggest these transitional periods contain
269 important photochemical signatures related to how symbionts cope with environmental stress.
270 Next, significant correlations for each bleaching response metric were further evaluated by
271 which photo-physiological metrics they reflect (Figure 4b,d). The most common photo-
272 physiological metrics significantly correlated with $\% \Delta$ in FvFm were τ_1^{ST} (28%), τ_2^{ST} (21%), and
273 antennae bed quenching (37%) while the most common for $\% \Delta$ in absorbance were the
274 absorbance cross section of PSII (39%), and Antennae Bed Quenching (36%).

275

276 **Predictive bleaching model evaluation:** For both bleaching response metrics, Random Forest -
277 based models were able to generate predictions which were significantly correlated with
278 observed trends in thermal bleaching responses (Figure 5b,e). Importantly, average bootstrapped
279 correlations between observed and predicted responses improved by incorporating additional
280 coral genotypes for model generation (Figure 5d,g). However, the bootstrapped-averaged
281 accuracy of predicting changes in Fv/Fm peaked with an R^2 value of 0.42 (± 0.018 CI, using 80
282 colonies for model testing). Accuracy in predicting changes in absorbance peaked at 0.33 (\pm
283 0.019 CI, using 80 colonies for model testing). While our R^2 plots suggest that model accuracy
284 may have improved with additional colonies used in training, the root mean squared error for
285 both metrics plateaued at roughly 23 and 19 (for Fv/Fm and absorbance respectively) with at
286 least 60 colonies used for model generation. When used to evaluate the average bleaching
287 response for the top and bottom ranked corals, model results for changes in Fv/Fm were between
288 67 and 71% accurate when at least 60 colonies were used to generate the model whereas results
289 for changes in absorbance peaked between 89-91% accurate when using at least 60 colonies for
290 model generation (Figure 5c,f).

291

292

293 **Discussion:** Our objective was to determine if easily measured, chlorophyll-a fluorescence-based
294 photo-physiological metrics could be used as a predictive tool for determining thermal tolerance
295 among different genotypes of the coral *Acropora palmata*. Identifying the degree of thermal
296 tolerance among different genotypes of the same coral species (or different corals) is a common
297 goal for many field studies and restoration initiatives (Voolstra et al., 2020; Voolstra et al., 2021;
298 Grummer et al., 2022; Evensen et al., 2023), yet current practices often require labor-intensive
299 experimental procedures, and the outcome is limited to only coral genotypes utilized in the study.
300 Establishing an Artificial Intelligence (AI) based approach where non-invasive measurements
301 can be used to predict thermal tolerance in novel colonies could remove a major bottleneck in
302 trait-based identification/selection of reef corals within basic and applied research settings.
303 Despite low correlation between our two bleaching response metrics (Fv/Fm and absorbance, Fig
304 2c), our phenomic-based dendrogram indicated that significant differences in bleaching
305 sensitivity existed across identified coral clusters (Figure 3) and suggests that underlying photo-
306 physiological data can be used to forecast thermal response within individual colonies. To test
307 this concept, we trained a Random Forest-based algorithm using algal phenotypic data, along
308 with bleaching response metrics to predict temperature tolerance in novel coral species (Figure
309 4-5). Such an approach can extend results of an experiment using data derived from bleaching
310 assays to train a model to infer information on novel coral genotypes, thereby vastly increasing
311 the value and utility of an individual experiment. High-throughput assays for identification of
312 thermal stress already rely on photochemical signatures to assess holobiont response (Voolstra et
313 al., 2020; Cunning et al., 2021) and our approach builds on these ideas through a massive
314 increase in the quantity and dimensionality of photosynthetic-data available.

315

316 **Phenotypic variability in bleaching response:** Bleaching response metrics were evaluated for
317 each coral genotype as a percent change between fragments from control and high temperature
318 treatments. Percent change in Fv/Fm varied broadly across individual genotypes yet collectively
319 averaged close to zero, indicating relative thermal stability of the symbionts (Figure 2a). While
320 *A. palmata* colonies *in situ* are commonly found to host *Symbiodinium fitti* (LaJeunesse, 2002),
321 colonies acclimated to land-based nurseries are often dominated by the more thermally tolerant
322 symbiont, *Durusdinium trenchii* (Gantt et al., 2023) and can retain this symbiosis even two years
323 after transplant back onto nearby reefs (Elder et al., 2023). Indeed, all the colonies used in our
324 experiment were previously housed in Mote's land-based nursery on Summerland Key (Mote
325 International Center for Coral Reef Research and Restoration) and likely also host the thermally
326 tolerant *D. trenchii* symbiont. Dominance by *D. trenchii* symbionts may explain the minimal
327 average reduction in Fv/Fm observed in response to 30 days of elevated temperatures. However,
328 high variability across genotypes (Figure 2a) may also suggest variability in symbiont dominance
329 across corals, possibly with more *S. fitti* dominated corals removed early in the experiment. In
330 contrast, changes in absorbance were more pronounced, with an average reduction of 23 percent.
331 Reductions in absorbance indicate a decline in photo pigmentation most likely associated with a
332 decline in symbiont cell density or chlorophyll *a* cell⁻¹. Despite discordant responses to thermal
333 stress, significant differences in the two bleaching response metrics were still found across
334 cluster-assigned phenotypes (Figure 3). These findings suggest a strong linkage between the
335 underlying photo-physiological poise of the coral colony and its resilience to future thermal
336 stress. Notably, such linkage extends past intra-colony variability as different ramets were used
337 for bleaching response (post-experiment) and photo-physiological assessment (pre-experiment),

338 highlighting the strength and potential utility of our technique within restoration/conservation
339 settings.

340 Concordant responses in Fv/Fm and absorbance found in prior studies assume that
341 bleaching is the result of thermal damage to the algal photosynthetic apparatus which induces the
342 over-production of radical oxygen species (ROS) which leach out into the host environment and
343 promote the signaling cascade that triggers cell expulsion (bleaching) (Weis, 2008; Hawkins &
344 Davy, 2012; Hawkins et al., 2015). Indeed, this thermal stress pathway is common among many
345 coral species, especially those considered thermally sensitive (Weis et al., 2008; Weis, 2008).

346 However, thermal stress may also reduce ROS scavenging activity by the host (Baird et al.,
347 2009), potentially leading to cell expulsion without any degradation to the photosynthetic
348 apparatus within the symbiont. Such discrepancies can lead to discordant interpretations of
349 bleaching tolerance based on what bleaching response metrics are utilized. Identifying what
350 physiological traits link to these separate responses is thus a critical step towards understanding
351 and predicting discordant patterns of thermal response, such as those observed here.

352

353 **Linkage between bleaching response and fluorescent signatures of photosynthetic poise:**

354 Photosynthesis to irradiance curves incrementally raise light intensity and monitor
355 photochemical response to understand light stress and acclimation mechanisms in marine algae
356 (Warner et al., 2010). Typically, each incremental light step is followed by a brief (20 second to 5
357 minute) period to allow for acclimation prior to measuring the photochemical response.

358 However, our protocol continuously records photochemical responses throughout our actinic
359 light protocol, capturing the acclimation phase as well (see Supplemental Figure S1). This
360 unique protocol thus allows for a higher-resolution understanding of rapid photochemical

361 changes in response to variable light. Notably, measurement periods immediately after
362 transitioning from dark (or low light) to higher light intensity were most correlated with
363 bleaching response metrics (Figure 4a,c). Prior studies have highlighted the importance of
364 understanding photochemical responses to quick transitions in light intensity (Allahverdiyeva &
365 Suorsa, 2015; Andersson et al., 2019) and variability is indeed notable across species of
366 Symbiodiniaceae (Hoadley et al., 2023). Better performance via smaller or faster acclimatization
367 to rapid changes in light may serve as a proxy for overall stress mitigation and may explain why
368 these metrics are more correlated with bleaching response as compared with subsequent
369 measurements of each light acclimation step. However, further research that focuses on
370 understanding the phenotypic variability within individual coral species (see Supplemental
371 Figure S1) or even across multiple coral and symbiont types will be required to understand if
372 such connections are prevalent across the Symbiodiniaceae family or if the relative importance
373 of individual photophysiological metrics or acclimatization periods differ across species or
374 environments.

375 Correlation matrices identified separate algal phenometrics as providing the best
376 correlations with the two bleaching response metrics (Fv/Fm and absorbance, Figure 4b-d).
377 Changes in reoxidation kinetics (τ_1^{ST} and τ_2^{ST}) represented the largest portion of metrics with a
378 significant correlation to temperature-induced changes in Fv/Fm (Figure 4b) and describe the
379 rate of electron transport through and the downstream of the PSII reaction center (Schuback et
380 al., 2021). Reoxidation kinetics are often used to identify stress or degradation at different sites
381 that may lower or inhibit photosynthetic capacity (Hoadley et al., 2021; Suggett et al., 2022;
382 Hoadley et al., 2023) and may explain the relationship with changes in Fv/Fm observed here
383 (Supplemental Table S2). In contrast, changes in absorbance due to high temperatures were most

384 linked to measurements of the absorption cross-section of PSII which reflects the size of light
385 harvesting compounds connected to a PSII reaction center. Given this direct connection to
386 photopigments, it is perhaps not surprising that this metric was well correlated with the percent
387 change in absorbance during thermal stress (Figure 4d, Supplemental Table S2). Additionally,
388 antennae bed quenching (ABQ) was also well correlated with both bleaching response metrics
389 (absorbance and Fv/Fm) and describes the reorientation of light harvesting pigments to dissipate
390 excess light energy. Changes in ABQ may therefor serve as an important proxy for the bleaching
391 response pathway which starts in the symbiont and leads to host driven cell expulsion.
392 Understanding what traits are best utilized to assess thermal response is critical for evaluating the
393 bleaching phenotype and our results here indicate that each response metric has unique sets of
394 biomarkers.

395

396 **AI-based predictive models for coral thermal resilience:** Model-based predictions using
397 genomic data have previously been applied to evaluating the thermal tolerance of individual
398 colonies of the coral *A. millepora* (Fuller et al., 2020). However, predictive accuracy was low
399 when based solely on host genetics and improved notably once information on environmental
400 conditions and symbiont dominance was included. On a larger spatial scale, survival rates of
401 coral larvae sourced from different locations have been used to predict which reefs along the
402 Great Barrier Reef are most likely to produce thermally tolerant corals (Quigley & van Oppen,
403 2022). Indeed, AI-based predictive models for coral research and restoration are already in use
404 but lack the high-throughput applicability required for scalable recommendations. Here, our
405 predictive pipeline first uses a correlation matrix to prioritize individual algal photo-
406 physiological metrics which are then fed into a Random Forest AI model and converted into

407 predictions of coral bleaching severity, concordant with experimentally produced observations
408 after long-term (4-weeks) exposure to high temperature stress (Figure 4 and 5). Although overall
409 average model strength peaked at 0.42 and 0.33 R^2 (for Fv/Fm and absorbance, respectively), the
410 use of additional colonies for initial training would improve accuracy. In addition, our results do
411 not incorporate colonies with the highest thermal sensitivity as those fragments were removed
412 prior to the end of the experiment and we were thus unable to capture their signal. The lack of
413 low tolerance corals within our training dataset may also have impacted the overall strength of
414 our predictive model. Model improvements through better training data, additional colonies or
415 incorporation of additional (easily measured) traits or measurement time points (to capture the
416 thermally sensitive individuals) could help strengthen our approach, providing a robust and
417 broadly applicable technique. Future work will also need to assess prediction accuracy across
418 coral species with and without thermally tolerant symbiont types to assess how discordant
419 responses (Figure 2) impact overall modeling efforts.

420 While our method largely focuses on the symbiont photophysiology to make predictions,
421 the coral host's influence on symbiont physiology is well documented (Enriquez et al., 2005;
422 Enríquez et al., 2017; Wangpraseurt et al., 2017; Xiang et al., 2020; Bollati et al., 2022) and can
423 be measured using chlorophyll-*a* fluorescence techniques (Hoadley et al., 2019). In this context,
424 our technique incorporates direct and indirect metrics of physiology from both the symbiont and
425 host, respectively. However, future predictive techniques that also incorporate additional and
426 direct host-centric physiological metrics such as GFP production or ROS scavenging could
427 further improve predictive accuracy and align with known host genomic traits that infer thermal
428 tolerance (Kenkel et al., 2013a; Dixon et al., 2015; Drury & Lirman, 2021; Rose et al., 2021;
429 Quigley & van Oppen, 2022).

430

431 **Conclusion:** By capturing a more complex fluorescent signature that includes rapid responses to
432 varying light using a low cost and open-source instrument, our approach allows for more
433 nuanced photo-physiological differences to be identified and then applied within our modeling
434 pipeline. Tools that increase our capacity to evaluate traits in a highly scalable and accessible
435 fashion are well suited for use towards ongoing coral reef restoration initiatives. Here,
436 chlorophyll-*a* fluorescence-based algal phenotyping combined with AI predictive models
437 converts our large physiological datasets into actionable products. The relatively low cost of our
438 instrumentation, along with the potential for broad application of trained models, could be highly
439 beneficial as a tool for rapidly selecting coral colonies with desirable traits. Although our focus
440 for this study was thermal tolerance, light, and water quality stress are also common challenges
441 for coral nurseries and outgrowth operations (Vardi et al., 2021; Voolstra et al., 2021) and
442 acclimatization to these stressors is also regulated through a combination of host and symbiont
443 physiology (Hennige et al., 2010; Suggett et al., 2012; Hoadley & Warner, 2017; Xiang et al.,
444 2020). Using a similar model training/testing approach, our phenotyping pipeline could prove
445 useful for informing on light and nutrient acclimatization traits as well. Future versions of our
446 multispectral/actinic light protocol could serve as a highly scalable and standardized means for
447 trait-based selection and comparison of coral/algae phenotypes across reef systems worldwide.

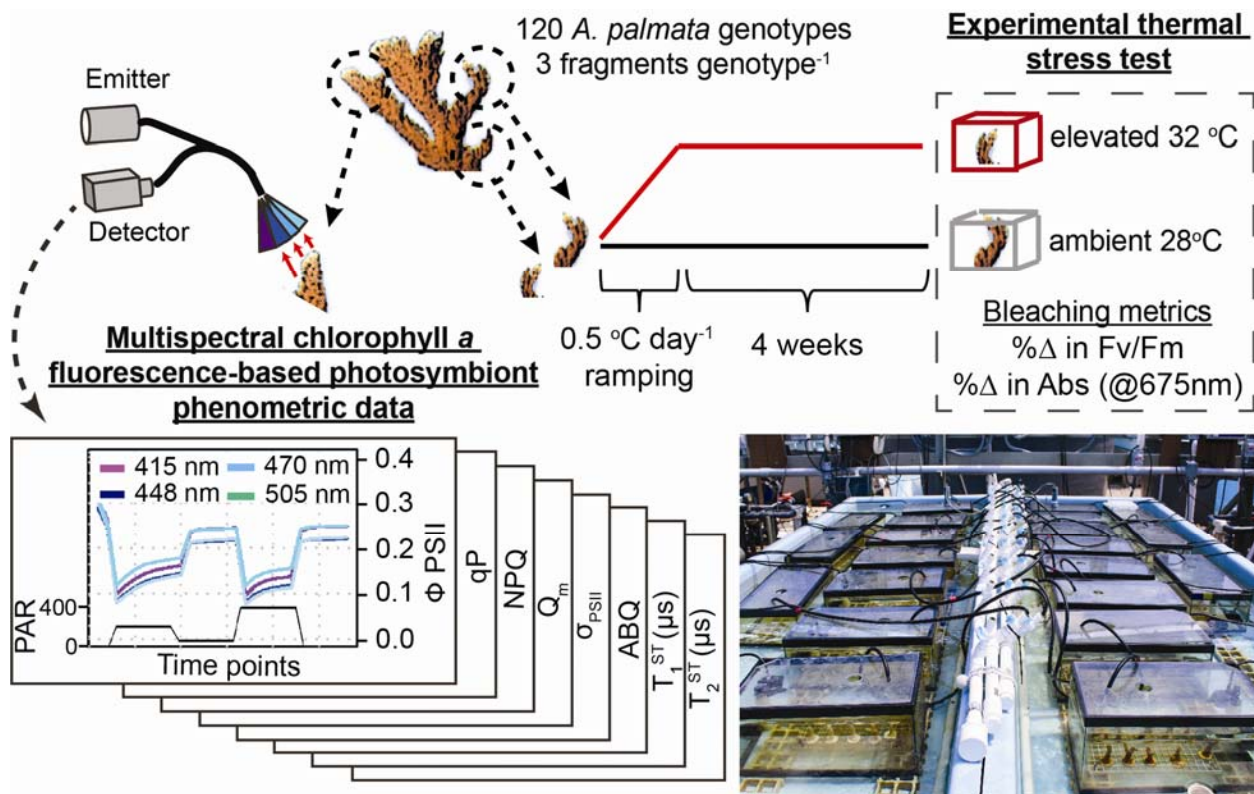
448 **Acknowledgements:** We thank the staff and interns at Mote's International Center for Coral
449 Reef Research and Restoration on Summerland Key, FL for their assistance and support.
450 Research activities were made possible through the Florida Fish and Wildlife Conservation
451 Commission (SAL-22-2406-SCRP and Florida Keys National Marine Sanctuary (FKNMS-2015-
452 163-A3) permits. The work was funded by the National Science Foundation, grant nos. 2054885
453 to K.D. Hoadley and the National Ocean and Atmospheric Administration, grant no.
454 NA21NMF4820300 to E.M and C.D.K. The authors declare no competing interests.

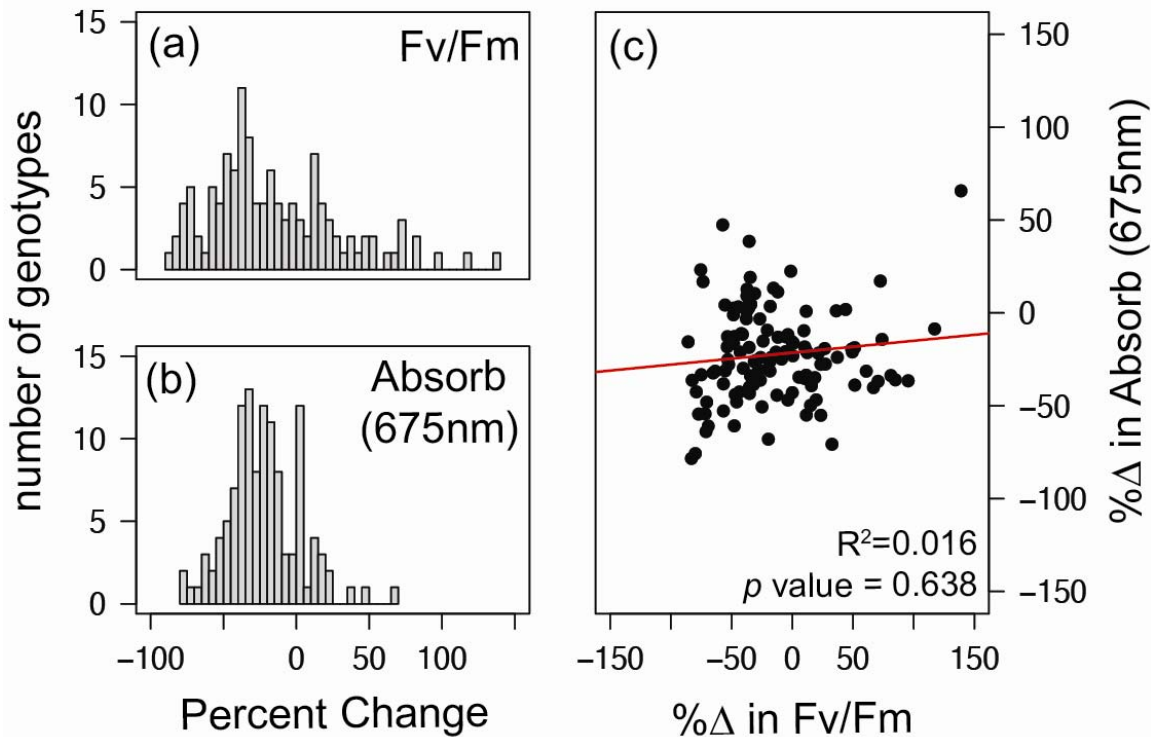
455

456 **Author Contributions:** C.D.K., E.M., and C.N.K. planned and designed the thermal bleaching
457 experiment. K.H developed the predictive model while G.L built the instrument. T.K., and
458 C.N.K. collected fragments, setup and conducted the thermal experiments. A.M., S.L., and S.D.
459 collected all phenotyping and bleaching response data. K.H. analyzed the data and wrote the
460 manuscript. All authors provided feedback on the manuscript. K.H. agrees to serve as the author
461 responsible for contact and ensures communication.

462

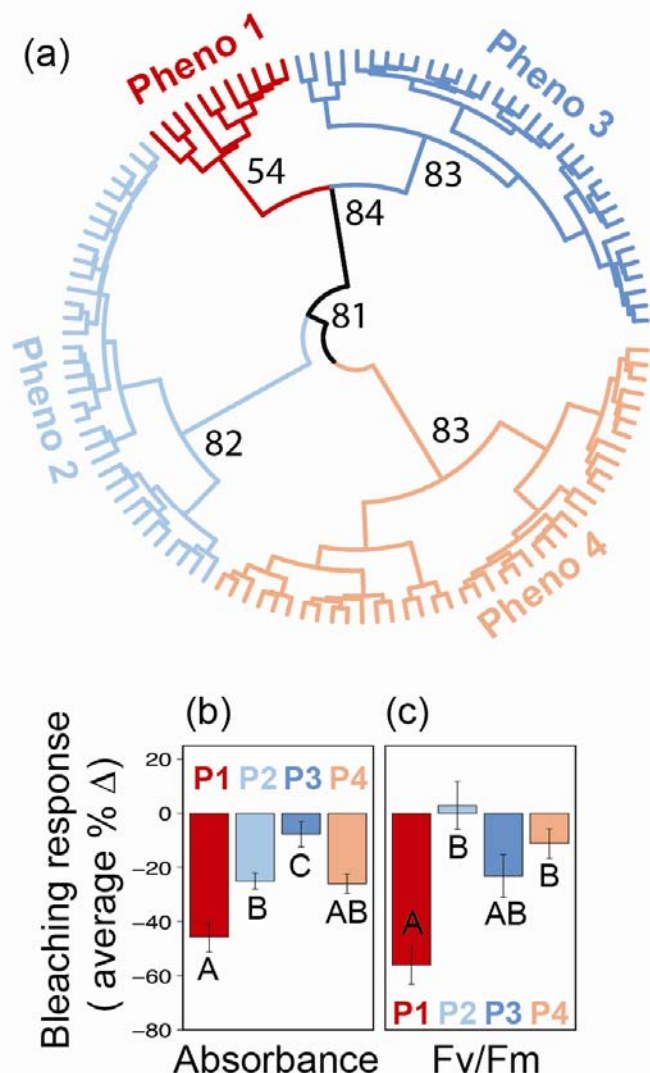
463 **Data Availability Statement:** All data needed to evaluate the conclusions in the paper are
464 present in the paper and/or the Supplementary Materials. Raw data and analytical scripts for
465 Figures 2 - 5 are available via github (khoadley/bleaching-prediction-2023).





479
480
481 **Figure 2 – Bleaching Response Metrics:** Results of the six-week thermal stress experiment
482 were characterized by recording Fv/Fm and Absorbance (at 675nm) measurements from each
483 coral colony and represented as the percent change between control and high temperature
484 conditions. Distribution of colony responses are displayed as separate histograms for % Δ in
485 Fv/Fm (a) and % Δ in Absorbance (b). Individual colony responses for both bleaching response
486 metrics are reflected in the correlation plot in panel (c) where the red line represents the best
487 linear fit to the data.
488

489

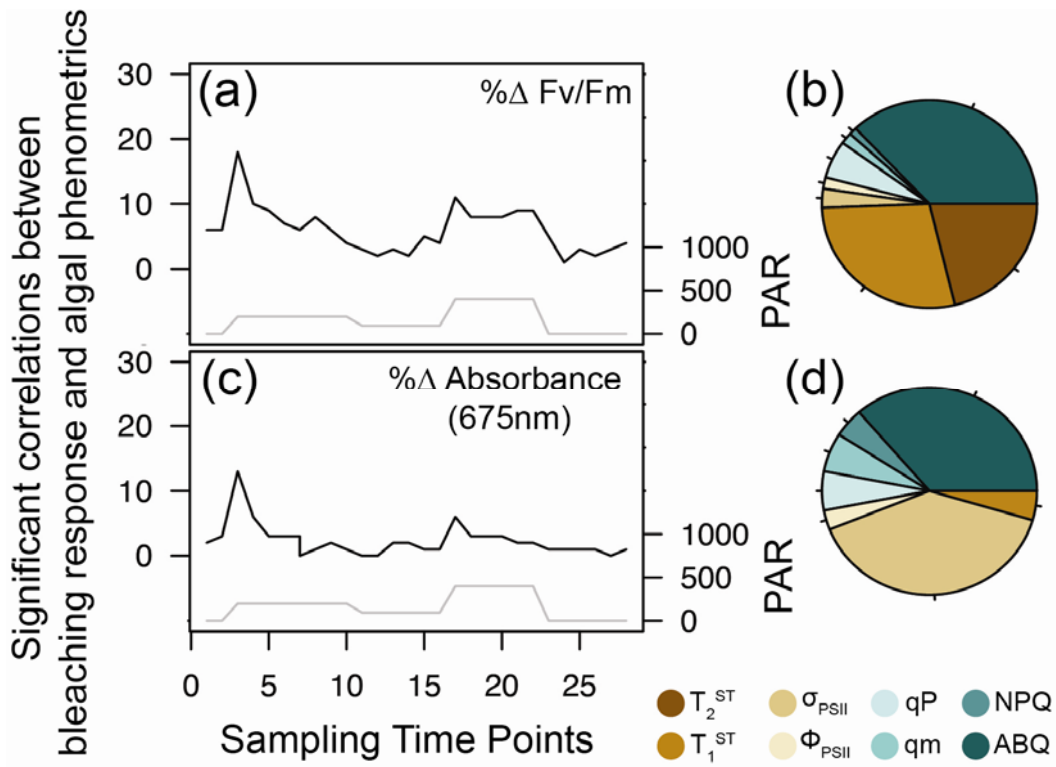


490

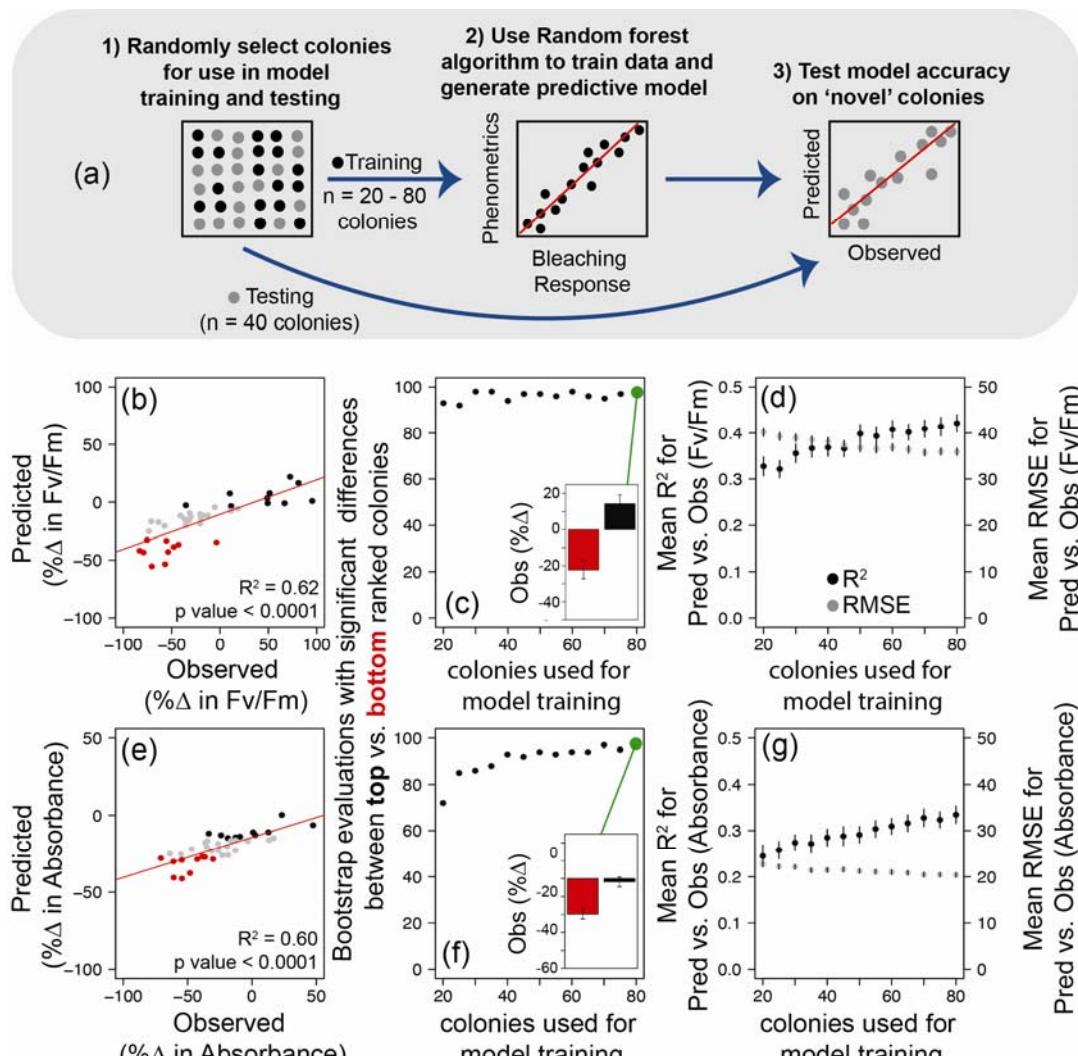
491

492 **Figure 3 – Coral Photosymbiont Phenotypic Variability:** Phenomic dendrogram (a) derived
493 from 716 photo-physiological metrics (autocorrelation values <0.99 Rho). The largest four
494 clusters are color coded (a). Bootstrap values are based on 10,000 iterations and are indicated for
495 major nodes delineating the four phenotypes. Bar graphs reflect the average \pm se for observed
496 temperature-induced changes in absorbance (b) and Fv/Fm (c) for the dendrogram's four
497 identified clusters/phenotypes. Letters under individual bars represent significant differences
498 across phenotypes as measured using a one-way ANOVA with Tukey-posthoc pairwise
499 comparisons. An extended version of this figure which includes mean traces for each photo-
500 physiological metric can be found in the supplementary document (Fig S1).

501



502
503
504 **Figure 4 – Phenomic vs. Bleaching Response Correlations:** A correlation matrix was used to
505 assess relationships between bleaching response metrics (% Δ in Fv/Fm and % Δ in absorbance)
506 and all algal photo-physiological metrics derived from the multispectral single-turnover
507 fluorometer. Panels (a) and (c) reflect significant correlations (spearman) between photo-
508 physiological metrics and % Δ in Fv/Fm or % Δ in absorbance (170 and 66 total/resulting metrics,
509 respectively) and are summarized according to the sampling time point (black line) from which
510 they are derived. The gray line in each figure reflects the PAR values for each step in the actinic
511 light protocol. Pie charts in panels (b) and (d) reflect the fraction of each algal metric
512 significantly correlated with % Δ in Fv/Fm and % Δ in absorbance, respectively.



532 **Table 1: Table of photo-physiological parameters:** Each defined parameter is represented by
533 spectrally dependent values at each sampling time point (Fig. 1).
534

Term	Definition	Units
Φ_{PSII}	Quantum yield of PSII. Measures the proportion of light energy captured by chlorophyll which is then utilized by the PSII reaction center for photosynthesis.	No units
qP	Photochemical quenching. Fraction of PSII reaction centers able to utilize light energy for photosynthesis.	No units
NPQ	Non-photochemical quenching. Light energy dissipation pathway describing the downregulation of PSII.	No units
σ_{PSII}	Absorption cross section of PSII. A measure of photon capture by light harvesting compounds connected to a PSII reaction center	nm ²
ABQ	Antennae Bed Quenching, Light energy dissipation pathway involving reorientation of light-harvesting compounds.	No units
Q_m	Excitation pressure over PSII	No units
τ_1^{ST}	Rate constant for reoxidation of the Q ^a site of the D1 protein within the PSII reaction center.	μ-seconds
τ_2^{ST}	Rate constant for reoxidation within and downstream of the plastoquinone pool	μ-seconds

535
536

537 **References:**

538

539 Abrego, D., Ulstrup, K.E., Willis, B.L., van Oppen, M.J. (2008). Species-specific interactions
540 between algal endosymbionts and coral hosts define their bleaching response to heat and
541 light stress. *Proc Biol Sci.* 275, 2273-2282.

542 Allahverdiyeva, Y., Suorsa..., M. (2015). Photoprotection of photosystems in fluctuating light
543 intensities. ... of experimental botany.

544 Andersson, B., Shen, C., Cantrell, M., Dandy..., D.S. (2019). The fluctuating cell-specific light
545 environment and its effects on cyanobacterial physiology. *Plant*

546 Baird, A.H., Bhagooli, R., Ralph, P.J., Takahashi, S. (2009). Coral bleaching: the role of the
547 host. *Trends in Ecology & Evolution.* 24, 16-20.

548 Barshis, D.J., Birkeland, C., Toonen, R.J., Gates, R.D., Stillman, J.H. (2018). High-frequency
549 temperature variability mirrors fixed differences in thermal limits of the massive coral
550 *Porites lobata*. *Journal of Experimental Biology.* 221, jeb188581.

551 Bollati, E., Lyndby, N.H., D'Angelo, C., Kühl, M., Wiedenmann, J., Wangpraseurt, D. (2022).
552 Green fluorescent protein-like pigments optimize the internal light environment in
553 symbiotic reef building corals. *Elife.* 11, e73521.

554 Boström-Einarsson, L., Babcock, R.C., Bayraktarov, E., Ceccarelli, D., Cook, N., Ferse, S.C.A.,
555 Hancock, B., Harrison, P., Hein, M., Shaver, E. (2020). Coral restoration—A systematic
556 review of current methods, successes, failures and future directions. *PloS one.* 15,
557 e0226631.

558 Caruso, C., Hughes, K., Drury, C. (2021). Selecting heat-tolerant corals for proactive reef
559 restoration. *Frontiers in Marine Science.* 8, 632027.

560 Cunning, R., Parker, K.E., Johnson-Sapp, K., Karp, R.F., Wen, A.D., Williamson, O.M., Bartels,
561 E., D'Alessandro, M., Gilliam, D.S., Hanson, G. (2021). Census of heat tolerance among
562 Florida's threatened staghorn corals finds resilient individuals throughout existing nursery
563 populations. *Proceedings of the Royal Society B.* 288, 20211613.

564 Dixon, G.B., Davies, S.W., Aglyamova, G.V., Meyer, E., Bay, L.K., Matz, M.V. (2015).
565 Genomic determinants of coral heat tolerance across latitudes. *Science.* 348, 1460-1462.

566 Drury, C., Lirman, D. (2021). Genotype by environment interactions in coral bleaching.
567 *Proceedings of the Royal Society B.*

568 Elder, H., Million, W.C., Bartels, E., Krediet, C.J., Muller, E.M., Kenkel, C.D. (2023). Long-
569 term maintenance of a heterologous symbiont association in *Acropora palmata* on natural
570 reefs. *The ISME Journal.* 17, 486-489.

571 Enriquez, S., Mendez, E.R., Iglesias-Prieto, R. (2005). Multiple scattering on corals enhances
572 light absorption by symbiotic algae. *Limnology and Oceanography.* 50, 1025-1032.

573 Enríquez, S., Méndez, E.R., Hoegh-Guldberg, O., Iglesias-Prieto, R. (2017). Key functional role
574 of the optical properties of coral skeletons in coral ecology and evolution. *Proceedings of
575 the Royal Society B: Biological Sciences.* 284, 20161667.

576 Evans, M.R., Norris, K.J., Benton, T.G. (2012). Predictive ecology: systems approaches.
577 *Philosophical Transactions of the Royal Society B: Biological Sciences.* 367, 163-169.

578 Evensen, N.R., Parker, K.E., Oliver, T.A., Palumbi, S.R., Logan, C.A., Ryan, J.S., Klepac, C.N.,
579 Perna, G., Warner, M.E., Voolstra, C.R. (2023). The Coral Bleaching Automated Stress
580 System (CBASS): A low-cost, portable system for standardized empirical assessments of
581 coral thermal limits. *Limnology and Oceanography: Methods.*

582 Fuller, Z.L., Mocellin, V.J.L., Morris, L.A., Cantin..., N. (2020). Population genetics of the coral
583 *Acropora millepora*: Toward genomic prediction of bleaching. *Science*.

584 Galili, T. (2015). dendextend: an R package for visualizing, adjusting and comparing trees of
585 hierarchical clustering. *Bioinformatics*.

586 Gantt, S.E., Keister, E.F., Manfroy, A.A., Merck, D.E., Fitt, W.K., Muller, E.M., Kemp, D.W.
587 (2023). Wild and nursery-raised corals: comparative physiology of two framework coral
588 species. *Coral Reefs*. 1-12.

589 Grummer, J.A., Booker, T.R., Matthey□Doret, R., Nietlisbach, P., Thomaz, A.T., Whitlock,
590 M.C. (2022). The immediate costs and long□term benefits of assisted gene flow in large
591 populations. *Conservation Biology*. e13911.

592 Hawkins, T.D., Davy, S.K. (2012). Nitric oxide production and tolerance differ among
593 Symbiodinium types exposed to heat stress. *Plant and Cell Physiology*. 53, 1889-1898.

594 Hawkins, T.D., Krueger, T., Wilkinson, S.P., Fisher, P.L., Davy, S.K. (2015). Antioxidant
595 responses to heat and light stress differ with habitat in a common reef coral. *Coral Reefs*.
596 DOI 10.1007/s00338-015.

597 Hennige, S.J., Smith, D.J., Walsh, S.-J., McGinley, M.P., Warner, M.E., Suggett, D.J. (2010).
598 Acclimation and adaptation of scleractinian coral communities along environmental
599 gradients within an Indonesian reef system. *Journal of Experimental Marine Biology and
600 Ecology*. 391, 143-152.

601 Hoadley, K.D., Lewis, A.M., Wham, D.C., Pettay, D.T., Grasso, C., Smith, R., Kemp, D.W.,
602 LaJeunesse, T.C., Warner, M.E. (2019). Host-symbiont combinations dictate the photo-
603 physiological response of reef-building corals to thermal stress. *Sci Rep*. 9, 9985.

604 Hoadley, K.D., Warner, M.E. (2017). Use of open source hardware and software platforms to
605 quantify spectrally dependent differences in photochemical efficiency and functional
606 absorption cross section. *Front Mar Sci*. doi: 10.3389/fmars.2017.00365.

607 Hoadley, K.D., Lockridge, G., McQuagge, A., Pahl, K.B., Lowry, S., Wong, S., Craig, Z., Petrik,
608 C., Klepac, C., Muller, E.M. (2023). A phenomic modeling approach for using chlorophyll-
609 a fluorescence-based measurements on coral photosymbionts. *Frontiers in Marine Science*.
610 10, 1092202.

611 Hoadley, K.D., Pettay, D.T., Dodge, D., Warner, M.E. (2016). Contrasting physiological
612 plasticity in response to environmental stress within different cnidarians and their
613 respective symbionts. *Coral Reefs*. 35, 1-14.

614 Hoadley, K.D., Pettay, D.T., Lewis, A., Wham, D., Grasso, C., Smith, R., Kemp, D.W.,
615 LaJeunesse, T., Warner, M.E. (2021). Different functional traits among closely related
616 algal symbionts dictate stress endurance for vital Indo□Pacific reef□building corals.
617 *Global Change Biology*.

618 Hughes, T.P., Anderson, K.D., Connolly, S.R., Heron, S.F., Kerry, J.T., Lough, J.M., Baird,
619 A.H., Baum, J.K., Berumen, M.L., Bridge, T.C. (2018). Spatial and temporal patterns of
620 mass bleaching of corals in the Anthropocene. *Science*. 359, 80-83.

621 Hughes, T.P., Kerry, J.T., Álvarez-Noriega, M., Álvarez-Romero, J.G., Anderson, K.D., Baird,
622 A.H., Babcock, R.C., Beger, M., Bellwood, D.R., Berkelmans, R. (2017). Global warming
623 and recurrent mass bleaching of corals. *Nature*. 543, 373.

624 Iglesias-Prieto, R., Beltran, V.H., LaJeunesse, T.C., Reyes-Bonilla, H., Thome, P.E. (2004).
625 Different algal symbionts explain the vertical distribution of dominant reef corals in the
626 eastern Pacific. *Proceedings of the Royal Society of London. Series B: Biological Sciences*.
627 271, 1757-1763.

628 Kenkel, C.D., Goodbody Gringley, G., Caillaud, D., Davies, S.W., Bartels, E., Matz, M.V.
629 (2013a). Evidence for a host role in thermotolerance divergence between populations of the
630 mustard hill coral (*Porites astreoides*) from different reef environments. *Molecular
631 Ecology*. 22, 4335-4348.

632 Kenkel, C.D., Matz, M.V. (2016). Gene expression plasticity as a mechanism of coral adaptation
633 to a variable environment. *Nat Ecol Evol*. 1, 14.

634 Kenkel, C.D., Meyer, E., Matz, M.V. (2013b). Gene expression under chronic heat stress in
635 populations of the mustard hill coral (*Porites astreoides*) from different thermal
636 environments. *Molecular Ecology*. 22, 4322-4334.

637 Kitchen, S.A., Von Kuster, G., Kuntz, K.L.V., Reich, H.G., Miller, W., Griffin, S., Fogarty,
638 N.D., Baums, I.B. (2020). STAGdb: a 30K SNP genotyping array and Science Gateway for
639 Acropora corals and their dinoflagellate symbionts. *Scientific reports*. 10, 12488.

640 Klepac, C.N., Eaton, K.R., Petrik, C.G., Arick, L.N., Hall, E.R., Muller, E.M. (2023). Symbiont
641 composition and coral genotype determines massive coral species performance under end-
642 of-century climate scenarios.

643 Kolber, Z., Prasil, O., Falkowski, P. (1998). Measurements of variable chlorophyll fluorescence
644 using fast repetition rate techniques: defining methodology and experimental protocols.
645 *Biochimica et Biophysica Acta (BBA) - Bioenergetics*. 1367, 88-107.

646 Kursar, M.B., Rudnicki, W.R. (2010). Feature selection with the Boruta package. *Journal of
647 statistical software*. 36, 1-13.

648 LaJeunesse, T. (2002). Community structure and diversity of symbiotic dinoflagellate
649 populations from a Caribbean coral reef. *Marine Biology*. 141, 387-400.

650 LaJeunesse, T.C., Parkinson, J.E., Gabrielson, P.W., Jeong, H.J., Reimer, J.D., Voolstra, C.R.,
651 Santos, S.R. (2018). Systematic revision of Symbiodiniaceae highlights the antiquity and
652 diversity of coral endosymbionts. *Current Biology*. 28, 2570-2580. e6.

653 Oxborough, K., Moore, C.M., Suggett..., D.J. (2012). Direct estimation of functional PSII
654 reaction center concentration and PSII electron flux on a volume basis: a new approach to
655 the analysis of Fast Repetition Rate *Limnology and*

656 Palumbi, S.R., Barshis, D.J., Traylor-Knowles, N., Bay, R.A. (2014). Mechanisms of reef coral
657 resistance to future climate change. *Science*. 344, 895-898.

658 Parkinson, J.E., Baker, A.C., Baums, I.B., Davies, S.W., Grottoli, A.G., Kitchen, S.A., Matz,
659 M.V., Miller, M.W., Shantz, A.A., Kenkel, C.D. (2020). Molecular tools for coral reef
660 restoration: beyond biomarker discovery. *Conservation Letters*. 13, e12687.

661 Parkinson, J.E., Banaszak, A.T., Altman, N.S., LaJeunesse, T.C., Baums, I.B. (2015).
662 Intraspecific diversity among partners drives functional variation in coral symbioses.
663 *Scientific reports*. 5, 15667.

664 Quigley, K.M., van Oppen, M.J.H. (2022). Predictive models for the selection of thermally
665 tolerant corals based on offspring survival. *Nature Communications*. 13, 1543.

666 Reichstein, M., Camps-Valls, G., Stevens, B., Jung, M., Denzler, J., Carvalhais, N. (2019). Deep
667 learning and process understanding for data-driven Earth system science. *Nature*. 566, 195-
668 204.

669 Rodriguez-Román, A., Hernández-Pech, X., Thomé, P.E., Enriquez, S., Iglesias-Prieto, R.
670 (2006). Photosynthesis and light utilization in the Caribbean coral *Montastraea faveolata*
671 recovering from a bleaching event. *Limnology and Oceanography*. 51, 2702-2710.

672 Rose, N.H., Bay, R.A., Morikawa..., M.K. (2021). Genomic analysis of distinct bleaching
673 tolerances among cryptic coral species. of the Royal

674 Schuback, N., Tortell, P.D., Berman-Frank, I., Campbell, D.A., Ciotti, A., Courtecuisse, E.,
675 Erickson, Z.K., Fujiki, T., Halsey, K., Hickman, A.E. (2021). Single-turnover variable
676 chlorophyll fluorescence as a tool for assessing phytoplankton photosynthesis and primary
677 productivity: opportunities, caveats and recommendations. *Frontiers in Marine Science*. 8,
678 690607.

679 Suggett, D.J., Goyen, S., Evenhuis, C., Szabó, M., Pettay, D.T., Warner, M.E., Ralph, P.J.
680 (2015). Functional diversity of photobiological traits within the genus *Symbiodinium*
681 appears to be governed by the interaction of cell size with cladal designation. *New*
682 *Phytologist*. 208, 370-381.

683 Suggett, D.J., Dong, L.F., Lawson, T., Lawrenz, E., Torres, L., Smith, D.J. (2012). Light
684 availability determines susceptibility of reef building corals to ocean acidification. *Coral*
685 *Reefs*. 32, 327-337.

686 Suggett, D.J., Nitschke, M.R., Hughes..., D.J. (2022). Toward bio□optical phenotyping of
687 reef□forming corals using Light□Induced Fluorescence Transient□Fast Repetition Rate
688 fluorometry. *Limnology and*

689 Suggett, D.J., Warner, M.E., Leggat, W. (2017). Symbiotic Dinoflagellate Functional Diversity
690 Mediates Coral Survival under Ecological Crisis. *Trends in Ecology and Evolution*. 32,
691 735-745.

692 Suzuki, R., Shimodaira, H. (2013). Hierarchical clustering with P-values via multiscale bootstrap
693 resampling. R package.

694 Team, R.C. (2017). R: a language and environment for statistical computing. R Foundation for
695 Statistical Computing, Vienna. <http://www.R-project.org>.

696 van Woesik, R., Shlesinger, T., Grottoli, A.G., Toonen, R.J., Vega Thurber, R., Warner, M.E.,
697 Marie Hulver, A., Chapron, L., McLachlan, R.H., Albright, R. (2022). Coral□bleaching
698 responses to climate change across biological scales. *Global Change Biology*.

699 Vardi, T., Hoot, W.C., Levy, J., Shaver, E., Winters, R.S., Banaszak, A.T., Baums, I.B.,
700 Chamberland, V.F., Cook, N., Gulko, D. (2021). Six priorities to advance the science and
701 practice of coral reef restoration worldwide. *Restoration Ecology*. 29, e13498.

702 Voolstra, C.R., Buitrago□López, C., Perna, G., Cárdenas, A., Hume, B.C.C., Rädecker, N.,
703 Barshis, D.J. (2020). Standardized short□term acute heat stress assays resolve historical
704 differences in coral thermotolerance across microhabitat reef sites. *Global Change Biology*.
705 26, 4328-4343.

706 Voolstra, C.R., Suggett, D.J., Peixoto, R.S., Parkinson, J.E., Quigley, K.M., Silveira, C.B.,
707 Sweet, M., Muller, E.M., Barshis, D.J., Bourne, D.G. (2021). Extending the natural
708 adaptive capacity of coral holobionts. *Nature Reviews Earth & Environment*. 2, 747-762.

709 Wangpraseurt, D., Holm, J.B., Larkum, A.W.D., Pernice, M., Ralph, P.J., Suggett, D.J., Kühl, M.
710 (2017). In vivo microscale measurements of light and photosynthesis during coral
711 bleaching: evidence for the optical feedback loop. *Frontiers in microbiology*. 8, 59.

712 Warner, M., Fitt, W., Schmidt, G. (1999). Damage to photosystem II in symbiotic
713 dinoflagellates: a determinant of coral bleaching. *Proceedings of the National Academy of*
714 *Sciences of the United States of America*. 96, 8007-8012.

715 Warner, M.E., Ralph, P.J., Lesser, M.P. (2010). Chlorophyll Fluorescence in Reef Building
716 Corals. In *Chlorophyll fluorescence in aquatic sciences: methods and applications*, D.J.
717 Suggett, O. Prasil, M. Borowitzka, eds. Springer), pp. 500.

718 Weis, V.M., Davy, S.K., Hoegh-Guldberg, O., Rodriguez-Lanetty, M., Pringle, J.R. (2008). Cell
719 biology in model systems as the key to understanding corals. *Trends in Ecology &*
720 *Evolution.* *23*, 369-376.

721 Weis, V.M. (2008). Cellular mechanisms of Cnidarian bleaching: stress causes the collapse of
722 symbiosis. *Journal of Experimental Biology.* *211*, 3059-3066.

723 Xiang, T., Lehnert, E., Jinkerson, R.E., Clowez, S., Kim, R.G., DeNofrio, J.C., Pringle, J.R.,
724 Grossman, A.R. (2020). Symbiont population control by host-symbiont metabolic
725 interaction in Symbiodiniaceae-cnidarian associations. *Nature communications.* *11*, 1-9.

726

727